Advances in Environmental Technology 10(4) 2024, 315-325.

Iranian Reasearch Organization for Science and Technology (IROST)

Advances in Environmental Technology

Journal home page: https://aet.irost.ir

Impact of TiO_2 and $CaCO_3$ nanoparticles and their incorporation in polysulfone composite membrane on photocatalytic degradation of RB 5

Sneha O [1], Arun M. Isloor [2*], Glanish Jude Martis [1], P. Satishkumar [2], Praveen S Mugali [1]

[1] Department of Post Graduation Studies in Organic Chemistry, Alva's College, Moodubidire 574 227, Karnataka, India.
[2] Membrane and Separation Technology Laboratory, Department of Chemistry, National Institute of Technology Karnataka, Surathkal, Mangalore 575 025, India.

ARTICLE INFO

Document Type:
Research Paper

Article history:
Received 25 June 2024
Received in revised form
17 September 2024
Accepted 22 September 2024

Keywords:
Nanoparticle,
Calcium Carbonate,
Titanium Dioxide,
Polysulfone Membrane

ABSTRACT

Contamination of water resources by dyes is a potential peril to humans and the ecosystem. Photocatalytic decomposition is one of the efficient ways to remove hazardous dyes present in water. $CaCO_3$ and TiO_2 nanoparticles have been synthesized from calcium chloride and sodium carbonate using a precipitation method and sol-gel technique, respectively. Synthesized $CaCO_3$ and TiO_2 nanoparticles were analysed using X-ray diffraction (XRD), ultraviolet visible (UV-Vis) spectroscopy, scanning electron microscopy (SEM), and energy dispersive X-ray spectroscopy (EDX). The experimental results showed that the synthesized $CaCO_3$ nanoparticles were of calcite and the TiO_2 nanoparticles of anatase. Polysulfone (PSF) composite membranes embedded with $CaCO_3$ and TiO_2 nanoparticles were prepared systematically. These synthesized nanoparticles and their embedded PSF membranes were effectively utilized for the photocatalytic decomposition of the reactive black 5 (RB 5) dye. 88.8% and 23.6% degradation of RB 5 dye was observed for TiO_2 and $CaCO_3$ nanoparticles, respectively. However, it was observed that the TiO_2 and $CaCO_3$ nanoparticle incorporated PSF membranes showed a lower photodegradation of 60.4% and 18.37%, respectively, due to the masking of the nanoparticles by the polymer matrix. The direct usage of the nanoparticles showed improved photodegradation properties.

1. Introduction

The availability of clean water has been declining at an alarming rate in recent years. It is known that dyes are one of the predominant pollutants of water. More than 10,000 dyes are commercially used in most industries, including paper, textile, plastic, etc. [1–3]. Dyes are not easily biodegradable, and most of them are highly carcinogenic [4]. When industrial effluents contaminated with dyes enter the water sources, they significantly damage the ecosystem and, in turn, human health as well [5]. Thus, the removal of dyes from water is of great need. The traditional methods to remove dyes from industrial effluents involve activated carbon, hydrogen peroxide, and other chemical reagents. However, these methods are not cost-effective and cannot meet the high purification standards [6]. In recent years, photocatalytic degradation has been noticed to be

*Corresponding author Tel.: +919448523990
E-mail: isloor@yahoo.com
DOI: 10.22104/aet.2024.6957.1907

advantageous in removal of toxic organic and inorganic contaminants from water [7–9].

Most of the active photocatalyst materials used are particles with <100nm diameter [10]. The use of these nanoparticles in removing dyes is considered less hazardous and has been a widely accepted method over the last decade [11]. Among those, TiO_2 nanoparticles have been found to be more effective due to their unique optical, dielectric, and catalytic properties. TiO_2 has a high photocatalytic efficiency due to its strong oxidation power and ability to generate reactive oxygen species (ROS) [12–16]. TiO_2 is chemically stable, non-toxic, and resistant to corrosion, making it durable in various environmental conditions. Another important nanoparticle that has been widely used in photocatalytic degradation is $CaCO_3$. These nanoparticles have been reported to have properties like high surface-to- volume ratio and ease of synthesis. Calcium carbonate is naturally abundant and inexpensive, making it an attractive material for large-scale applications. Another important factor is it is biocompatible and non-toxic, which is beneficial for environmental and health safety. Apart from these, it has the unique ability to exist in a variety of morphologies, which makes it an ideal material for industrial and biomedical applications [17]. Both TiO_2 and $CaCO_3$ nanoparticles, due to their nano size, lead to the overall increase in the surface area of the photocatalyst, resulting in the augmentation of active sites, thereby increasing the specific site for the photocatalytic degradation process [18].

In the area of water purification and separation, membranes have gained exceptional attention over the last few years due to their low energy demand and efficacy [19]. A wide variety of polymers, such as Polysulfone [20], polyether sulfone [21], polyphenyl sulfone [22], polyvinylidene fluoride [23], polyimide [24], and many others, have been utilized in the fabrication of membranes. Among all the polymers, Polysulfone exhibits appreciable properties, such as high chlorine resistance, thermal stability, and wide pH tolerance [25]. The properties of the polymers can be greatly enhanced according to the need of the application by incorporating inorganic nanoparticles [26]. A large pool of inorganic additives has been utilized for this purpose, including TiO_2 [27], calcium carbonate [28], tin oxide [22], zirconium oxide [29], cerium oxide [30], ferric oxide [31], aluminium oxide, silicates [32], etc. Erusappan and group members fabricated a TiO_2 nanoparticle incorporated PVDF membrane for photocatalytic degradation of Congo red and reactive yellow 145 [33]. The fabricated TiO_2-PVDF membrane showed 67% and 77% decolourization of Congo red and reactive yellow 145, respectively. Alaoui and co-workers prepared an anatase TiO_2-PVDF membrane for a photocatalytic dye removal study [34]. The fabricated anatase TiO_2-PVDF membrane displayed a photocatalytic degradation rate of 6.1 and 2.4 μmol L^{-1} min^{-1} for indigo carmine and brilliant green dyes, respectively. The literature shows that nanoparticle embedded membranes have been extensively used in the photocatalytic degradation of various dyes since they are less hazardous and less expensive compared to other methods.

The purpose of this work is to synthesize TiO_2 and $CaCO_3$ nanoparticles and analyse their photocatalytic degradation strength with respect to reactive black 5 dye in two different ways. The first one is by directly taking the aqueous solution of the synthesized nanoparticles, and the second one is by fabricating TiO_2 and $CaCO_3$ nanoparticle incorporated Polysulfone nanocomposite membranes.

2. Materials and Methods

2.1. Synthesis of TiO_2 nanoparticles (TNP)

TiO_2 nanoparticles (Nps) were synthesized using the sol-gel method. 12 mL of titanium tetraisopropoxide [$Ti(OC_3H_7)_4$] was added to 10ml of isopropanol. After the sol of TiO_2 was prepared, 150ml of water and 5ml of acetic acid were poured into the tetraisopropoxide and isopropanol mixture; the solution was heated at 80°C for 3 hrs with constant stirring. 1 mL of conc. HNO_3 was added to prevent the clustering of particles present in the sol; then, it was dried in the oven at 100°C for 10 hrs [35].

2.2. Synthesis of $CaCO_3$ nanoparticles (CCNP)

$CaCO_3$ nanoparticles were synthesized by reacting calcium chloride ($CaCl_2$) and sodium carbonate (Na_2CO_3). Calcium chloride and sodium carbonate were used without further purification and were of analytical grade. Calcium chloride (0.01M) and

sodium carbonate (0.01M) solutions were separately prepared using 50ml of distilled water. An aqueous solution of sodium carbonate was added to the calcium chloride solution with constant stirring. After continuous stirring for 30 minutes, a white precipitate was obtained. The obtained precipitate was filtered and washed with distilled water multiple times. White $CaCO_3$ Nps obtained were kept at 105°C in a hot air oven for 1 hr and finally stored in a vacuum [18].

2.3. Photocatalytic degradation of dye using nanoparticles

150mg of CCNP was weighed accurately and added to 300ml of 10ppm RB 5 solution. The structure of RB 5 dye is given in Figure 1 [36]. The solution was sonicated for 30 min and transferred to a photocatalytic reactor. A sample was collected periodically at 15 min intervals and centrifuged for 20 min at 3000 rpm. The supernatant solution was separated and subjected to UV-Visible spectroscopic analysis. A similar procedure was performed using TiO_2 Nps and analysed using UV-Visible spectroscopic analysis.

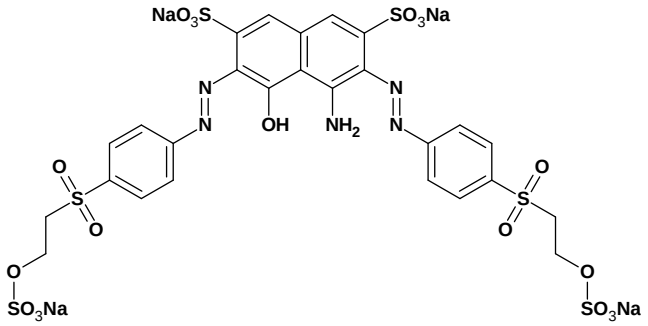

Fig. 1. The Chemical structure of Reactive Black 5 dye

2.4. Preparation of nanoparticles incorporated PSF composite membranes

0.02g of CCNP was accurately weighed and added to 7.48g of N-Methyl-2-Pyrrolidone (NMP). The above mixture was sonicated until the particles were completely dispersed. 0.5g of polyethylene glycol (PEG) 600 and 2g of PSF pellets were added and stirred for 24 hrs at 350 rpm (55°C). The viscous solution was then cast over a glass plate with a thickness of about 0.1 mm, and the glass plate was immersed in a water bath overnight [28]. Following a similar procedure, the TiO_2 incorporated PSF membrane was also prepared. The fabricated membranes obtained were used for photocatalytic degradation of RB 5.

2.5. Characterization of synthesized nanoparticles

The successful synthesis of CCNP and TNP was confirmed by XRD analysis (Rigaku Miniflex [5th generation]). The diffraction peaks obtained from the instruments were studied to understand the crystal structure of the synthesized nanoparticles. The size and surface morphology of the synthesized CCNP and TNP were determined using a ZEISS EVO MA18 SEM instrument. Oxford EDS (X-act) was utilized to determine the surface elemental composition of CCNP and TNPs. The amount of dye degradation was quantified with the help of UV-Visible spectroscopy. Both the feed and the reaction mixture were collected separately at different time intervals, and the concentration of dye molecules in each was determined in terms of absorbance using a UV-Visible spectrophotometer.

3. Results and Discussion

3.1. XRD analysis

An XRD study was carried out to determine the crystallographic structure of the nanoparticles. The data obtained from the XRD analysis of CCNP is shown in Figure 2 and indicate that the nanoparticles are scheduled to the rhombohedral phase. The peaks of the sample produced at the 22.88°, 29.26°, 35.81°, 39.2°, 43.03°, 48.26°, 57.24°, and 64.38° angles were related to planes (012), (104), (110), (113), (202), (116), (122), and (125), respectively. The XRD pattern obtained corresponded to crystalline polymorph calcite. The other two crystal types were aragonite and vaterite. The calcite type is the most stable polymorph of calcium carbonate and exhibits a rhombohedral shape. The calcite form shows high birefringence and, thus, is commonly used in optical applications.

The XRD analysis of TNP is shown in Figure 3. The peaks found at the 25.06°, 37.7°, 47.76°, 54.8°, 62.52°, and 70° angles are labeled to planes (011), (112), (020), (121), (024), and (220), respectively. These peaks confirmed the successful synthesis of the anatase crystal form of TiO_2. The other two

crystal types were rutile and brookite. The anatase crystal form exhibited excellent photocatalytic activity and was more stable at a lower temperature. A tetragonal structure with a high surface area was another characteristic feature of the anatase crystal form of TiO_2.

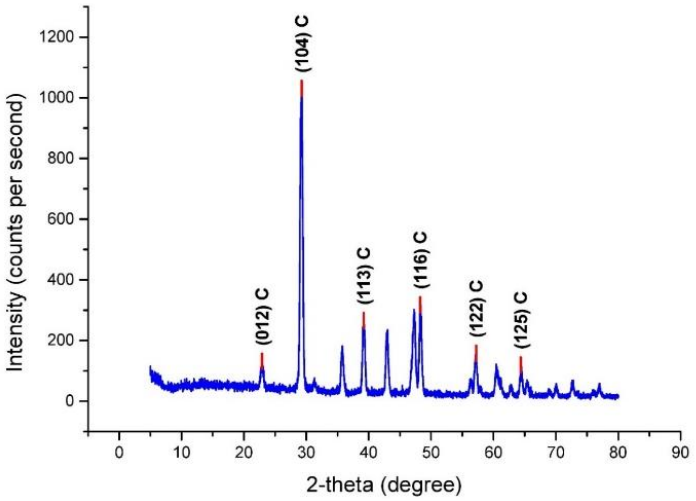

Fig. 2. XRD pattern of $CaCO_3$ nanoparticles.

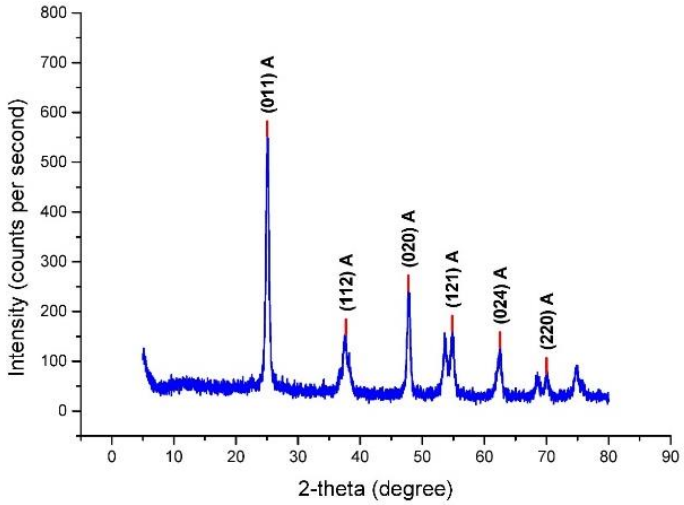

Fig. 3. XRD pattern of TiO_2 nanoparticles.

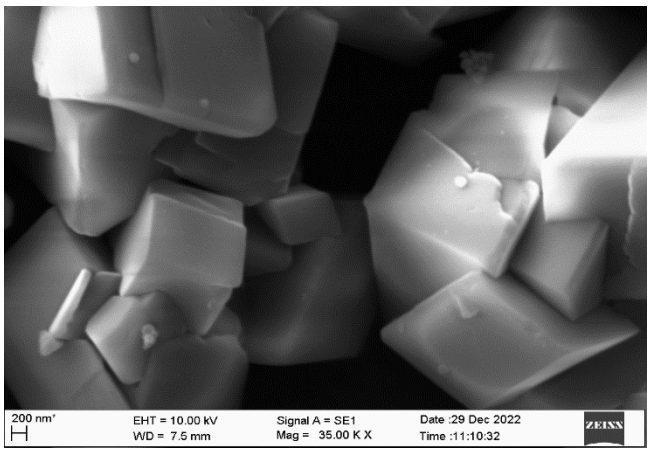

Fig. 4a. SEM image of $CaCO_3$ nanoparticles (area 1)

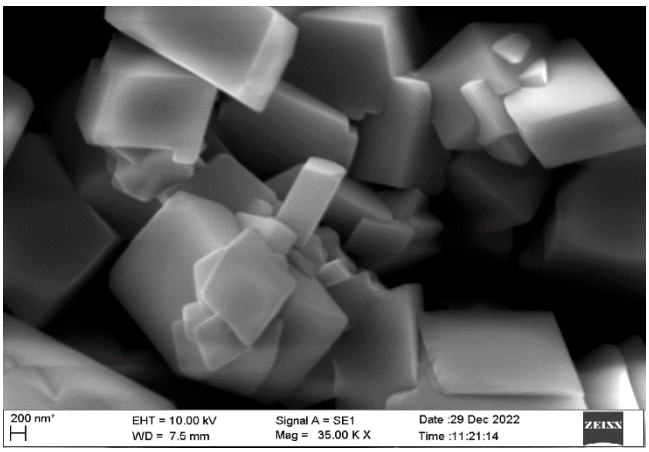

Fig. 4b. SEM Image of $CaCO_3$ nanoparticles (area 2)

3.2. SEM and EDAX study

The shape and morphology of CCNP and TNP were clearly observed using SEM micrographs. Figure 4 depicts the SEM micrographs of CCNP. Micrographs were taken in magnifications of 35,000x and at a working distance of 7.5mm. The SEM images confirmed that the synthesized CCNP was in the nanometre range. The SEM images clearly showed the rhombohedral shape of the synthesized CCNPs, which is the peculiar morphology of calcite.

The elemental composition of the synthesized CCNP was analysed using EDX (Figure 5). The peaks in the EDX spectrum confirmed the presence of elements such as calcium, carbon, and oxygen. The peaks at 0.34 KeV and 3.69 KeV corresponded to calcium and were of the Kα line and Lα line, respectively. The presence of carbon was indicated by a peak observed at 0.28 KeV. The peak at 0.5 KeV was assigned for oxygen. The absence of any other peak confirmed that the synthesized nanoparticles were pure without any impurities. The weight percent of these elements was also determined.

Figure 6 represents the SEM micrographs of TNP taken in different areas. The micrographs were taken in magnifications of 35,000x and at a working distance of 7.5mm. The SEM images confirmed that the synthesized CCNP was in the nanometre range. In SEM images, the tetragonal crystal structure appeared as spherical and had irregular shapes with a rough surface. The EDAX enabled the elemental analysis of TNP, which is depicted in Figure 7. The EDAX data confirmed that the synthesized TNP consisted of only titanium and oxygen elements and was free from contamination. The peaks observed at 0.45 KeV and 4.51 KeV corresponded to the Lα and Kα lines of titanium. The presence of oxygen was denoted by the peak observed at 0.52 KeV. The weight % of titanium and oxygen was 59.75% and 40.2%, respectively.

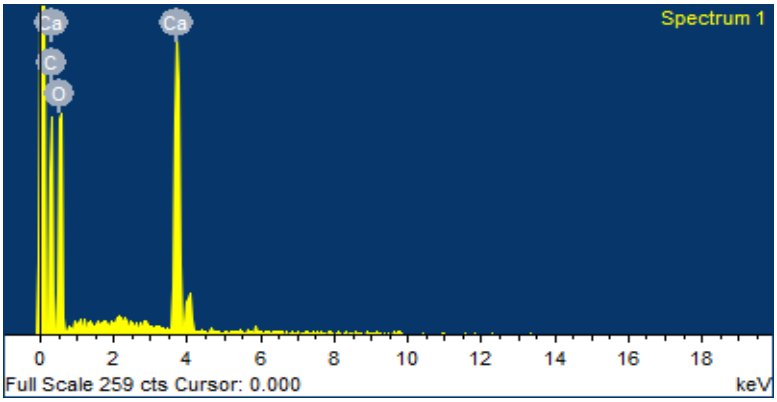

Fig. 5. EDAX spectrum of CCNP

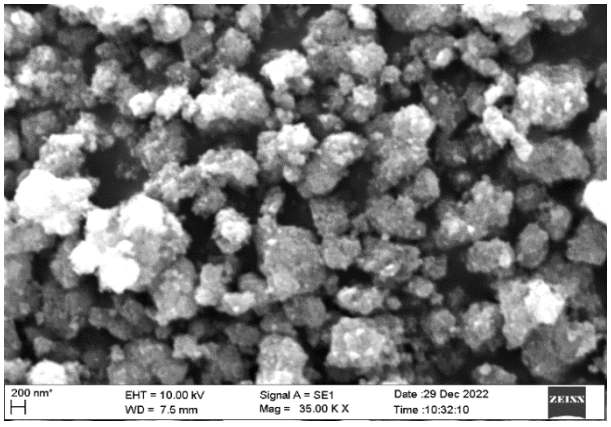

Fig. 6a. SEM image of TiO_2 nanoparticles (area 1)

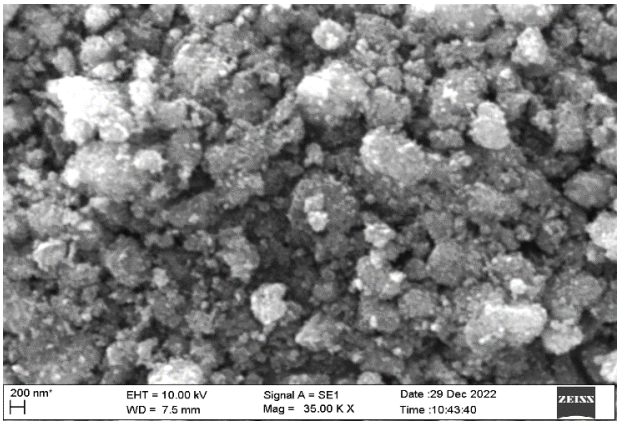

Fig. 6b. SEM image of TiO_2 nanoparticles (area 2)

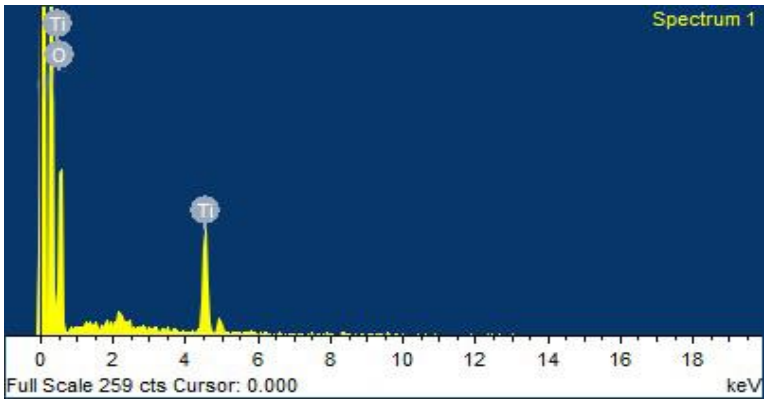

Fig. 7. EDAX spectrum of TiO_2 nanoparticles

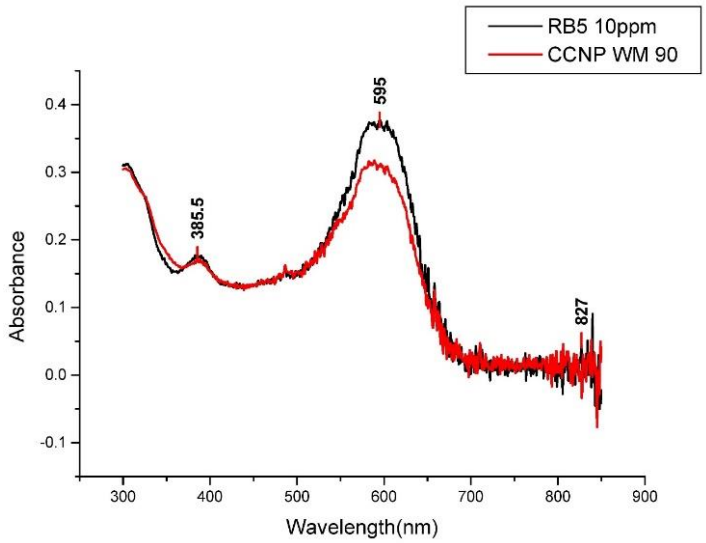

Fig. 8. Effect of $CaCO_3$ nanoparticles on RB 5 dye degradation

3.3. *Dye degradation study*

Photocatalysis is a process that utilizes light to accelerate a chemical reaction. Regarding the degradation of dyes, photocatalysis can be a highly effective method. When the nanoparticles are exposed to light, particularly UV light, they absorb photons. The absorbed energy excites the electrons from the valence band to the conduction band, creating electron-hole pairs. The excited electrons and holes can react with oxygen and water molecules in the surrounding environment to form reactive oxygen species, such as hydroxyl radicals (•OH) and superoxide anions (O_2^-). These ROS are highly reactive and can break down dye molecules into smaller, less harmful compounds through oxidative reactions. UV-Visible spectroscopic analysis was carried out for the samples collected at regular time intervals of 15 minutes and for the feed solution of RB 5 dye. Figure 8 illustrates the photocatalytic degradation of RB 5 (10 ppm) at 90 min using calcium carbonate without a membrane, which is represented as CCNP WM. The degradation of RB 5 using CCNP WM was slow and observed at 90 min of reaction. RB 5 dye degradation was observed at 595 nm, accounting for 23.68% degradation.

Figure 9 emphasizes the photocatalytic degradation of RB 5 (1.3 ppm) at different time intervals using the CCNP embedded PSF composite membrane. It was observed that the degradation of RB 5 using the CCNP incorporated PSF membrane was less efficient compared to CCNP

WM and showed 18.37% degradation of RB 5 dye. This was due to the fact that the nanoparticles were masked by the polymer matrix in CCNP WM.

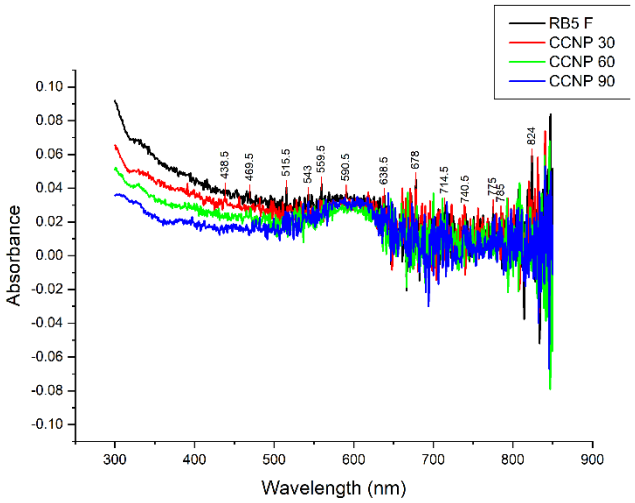

Fig. 9. Effect of $CaCO_3$ nanoparticles incorporated PSF membrane on degradation RB 5 dye.

Figure 10 depicts the photocatalytic degradation of RB 5 dye (10ppm) using TiO_2 nanoparticles without the membrane, which is represented as TNP WM. From this graphical analysis, it was evident that TNP was an excellent photocatalyst for the degradation of RB 5, showing a significant peak at 595 nm, referring to 88.88% degradation of RB 5 dye.

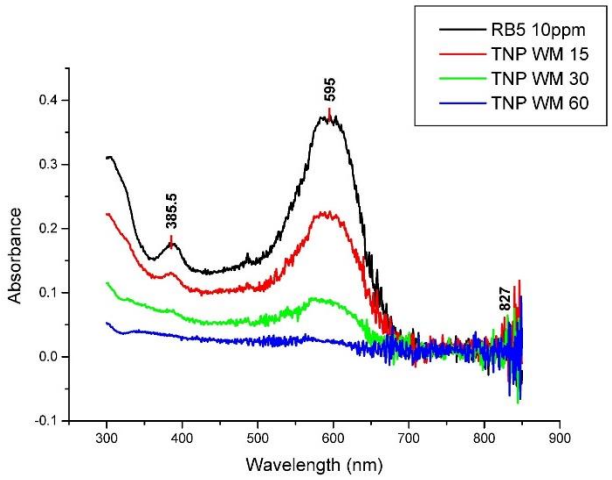

Fig. 10. Effect of TiO_2 nanoparticles on degradation of RB 5 dye.

Figure 11 represents the photocatalytic degradation of RB 5 (1.3ppm) using the TNP embedded PSF composite membrane. The TNP incorporated membrane was found to be less efficient in the degradation of RB 5 compared to TNP WM. However, it successfully degraded 60.45% of RB 5 dye from the water.

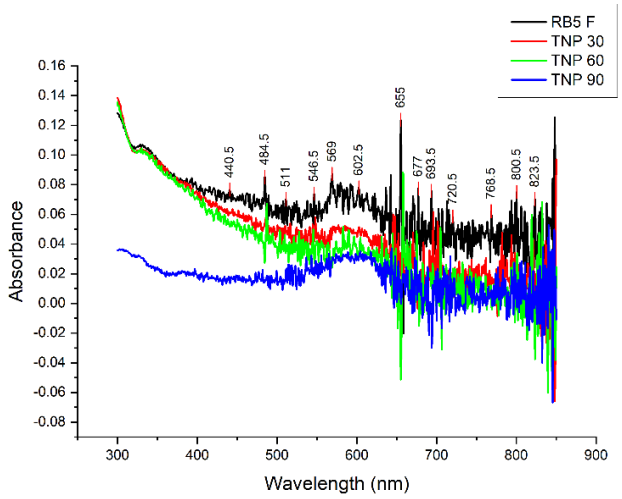

Fig. 11. Effect of TiO2 nanoparticles incorporated polysulfone membrane on RB 5 dye degradation

Photographs showing the RB 5 feed solution and samples collected at various time intervals are shown in Figures 12 and 13. The photographs depict the degradation of 10ppm RB5 dye degradation upon photocatalytic reaction using TiO_2 nanoparticles and $CaCO_3$ nanoparticles, respectively. According to the figure, the degradation of the dyes was enhanced with an increase in UV light exposure time on the dye solution. Both the TiO_2 and $CaCO_3$ nanoparticles absorbed the UV light, which constituted a small portion of the solar spectrum. Coupling it with other elements could enhance their overall efficiency and broaden their absorption spectrum.

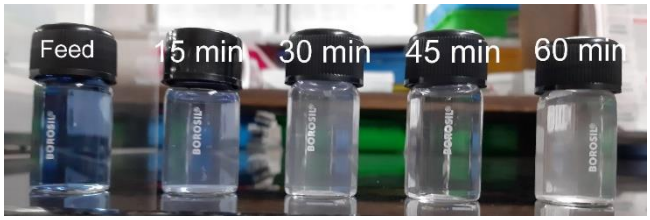

Fig. 12. Photograph of RB 5 Dye feed and samples collected at different time intervals in TiO_2 photocatalysis.

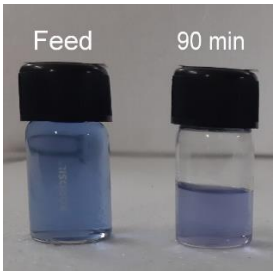

Fig. 13. Photograph of RB 5 Dye feed and samples collected at 90 minutes time in $CaCO_3$ photocatalysis.

The photographs of 1.3 ppm RB 5 dye degradation with TNP and CCNP with PSF membranes is shown in Figures 14 and 15, respectively.

Fig. 14. Photograph of RB 5 Dye degradation using TNP-PSF membrane

Fig. 15. Photograph of RB 5 Dye degradation using CCNP-PSF membrane

4. Conclusion

This study demonstrated the preparation of $CaCO_3$ nanoparticles, TiO_2 nanoparticles, and PSF composite membranes incorporated with $CaCO_3$ and TiO_2 nanoparticles. The successful synthesis of both nanoparticles was confirmed by its characterization using SEM and XRD techniques. The photocatalytic activity of these nanoparticles was studied by degrading the RB 5 solution exposed to UV light. It was seen that both $CaCO_3$ nanoparticles and their composite membranes were not very effective in degrading RB 5 dye. This was due to the fact that the nanoparticles were masked by the polymer matrix, lowering its activity. However, TNP was found to be an excellent photocatalyst in the degradation of RB 5 dye. Compared to TNP with membranes, TNP without membranes was found to be more effective. This study concluded that TiO_2 nanoparticles were a better photocatalyst in the degradation of RB 5 compared to $CaCO_3$.

Acknowledgements

Authors are grateful to the National Institute of Technology Karnataka (NITK), Surathkal, India, for the lab and instrument facility.

References

[1] Teng, T. T., & Low, L. W. (2012). Removal of Dyes and Pigments from Industrial Effluents. In S. K. Sharma & R. Sanghi (Eds.), *Advances in Water Treatment and Pollution Prevention* (pp. 65–93). Dordrecht: Springer Netherlands. https://doi.org/10.1007/978-94-007-4204-8_4

[2] Hebbar, R. S., Isloor, A. M., Inamuddin, Abdullah, Mohd. S., Ismail, A. F., & Asiri, A. M. (2018). Fabrication of polyetherimide nanocomposite membrane with amine functionalised halloysite nanotubes for effective removal of cationic dye effluents. *Journal of the Taiwan Institute of Chemical Engineers*, *93*, 42–53. https://doi.org/10.1016/j.jtice.2018.07.032

[3] Satishkumar, P., Isloor, A. M., Rao, L. N., & Farnood, R. (2024). Fabrication of 2D Vanadium MXene Polyphenylsulfone Ultrafiltration Membrane for Enhancing the Water Flux and for Effective Separation of Humic Acid and Dyes from Wastewater. *ACS Omega*. https://doi.org/10.1021/acsomega.3c10078

[4] Ikram, M., Raza, A., Imran, M., Ul-Hamid, A., Shahbaz, A., & Ali, S. (2020). Hydrothermal Synthesis of Silver Decorated Reduced Graphene Oxide (rGO) Nanoflakes with Effective Photocatalytic Activity for Wastewater Treatment. *Nanoscale Research Letters*, *15*(1), 95. https://doi.org/10.1186/s11671-020-03323-y

[5] Elbakry, S., Ali, M. E. A., Abouelfadl, M., Badway, N. A., & Salam, K. M. M. (2022). Photocatalytic degradation of organic compounds by TFC membranes functionalized with Ag/rGO nanocomposites. *Journal of Photochemistry and Photobiology A: Chemistry*, *430*, 113957. https://doi.org/10.1016/j.jphotochem.2022.113957

[6] Neppolian, B., Sakthivel, S., Arabindoo, B., Palanichamy, M., & Murugesan, V. (1999). Degradation of textile dye by solar light using TiO_2 and ZnO photocatalysts. *Journal of Environmental Science and Health, Part A*, *34*(9), 1829–1838. https://doi.org/10.1080/10934529909376931

[7] Pelizzetti, E., Minero, C., Borgarello, E., Tinucci, L., & Serpone, N. (1993). Photocatalytic activity and selectivity of titania colloids and particles prepared by the sol-gel technique: photooxidation of phenol and atrazine. *Langmuir*, *9*(11), 2995–3001. https://doi.org/10.1021/la00035a043

[8] Ollis, D. F. (2000). Photocatalytic purification and remediation of contaminated air and water. *Comptes Rendus de l'Académie des Sciences - Series IIC - Chemistry*, *3*(6), 405–411. https://doi.org/10.1016/S1387-1609(00)01169-5

[9] Bahnemann, D., Cunningham, J., Fox, M. A., Pelizzetti, E., Pichat, P., & Serpone, N. (1994). Photocatalytic Treatment of Waters. In *Aquatic and Surface Photochemistry*. CRC Press.

[10] Kostedt, Ismail, A. A., & Mazyck, D. W. (2008). Impact of Heat Treatment and Composition of ZnO–TiO2 Nanoparticles for Photocatalytic Oxidation of an Azo Dye. *Industrial & Engineering Chemistry Research*, *47*(5), 1483–1487. https://doi.org/10.1021/ie071255p

[11] Mehta, M., Sharma, M., Pathania, K., Jena, P. K., & Bhushan, I. (2021). Degradation of synthetic dyes using nanoparticles: a mini-review. *Environmental Science and Pollution Research*, *28*(36), 49434–49446. https://doi.org/10.1007/s11356-021-15470-5

[12] Barbé, C. J., Arendse, F., Comte, P., Jirousek, M., Lenzmann, F., Shklover, V., & Grätzel, M. (1997). Nanocrystalline Titanium Oxide Electrodes for Photovoltaic Applications. *Journal of the American Ceramic Society*, *80*(12), 3157–3171. https://doi.org/10.1111/j.1151-2916.1997.tb03245.x

[13] Monticone, S., Tufeu, R., Kanaev, A. V., Scolan, E., & Sanchez, C. (2000). Quantum size effect in TiO_2 nanoparticles: does it exist? *Applied Surface Science*, *162–163*, 565–570. https://doi.org/10.1016/S0169-4332(00)00251-8

[14] Boujday, S., Wünsch, F., Portes, P., Bocquet, J.-F., & Colbeau-Justin, C. (2004). Photocatalytic and electronic properties of TiO2 powders elaborated by sol–gel route and supercritical drying. *Special issue dedicated to Prof. Dr. H. Tributsch on the occasion of his 60th birthday*, *83*(4), 421–433. https://doi.org/10.1016/j.solmat.2004.02.035

[15] Carp, O., Huisman, C. L., & Reller, A. (2004). Photoinduced reactivity of titanium dioxide. *Progress in Solid State Chemistry*, *32*(1), 33–177. https://doi.org/10.1016/j.progsolidstchem.2004.08.001

[16] Ruiz, A. M., Sakai, G., Cornet, A., Shimanoe, K., Morante, J. R., & Yamazoe, N. (2004). Microstructure control of thermally stable TiO_2 obtained by hydrothermal process for gas sensors. *The 17th Euopean Conference on Solid-State Transducers, University of Minho, Guimares, Portugal, September 21-24, 2003*, *103*(1), 312–317. https://doi.org/10.1016/j.snb.2004.04.061

[17] Fadia, P., Tyagi, S., Bhagat, S., Nair, A., Panchal, P., Dave, H., Singh, S. (2021). Calcium carbonate nano- and microparticles: synthesis methods and biological applications. *3 Biotech*, *11*(11), 457. https://doi.org/10.1007/s13205-021-02995-2

[18] Jeyasubramanian, K., & Muthuselvi, M. (2020). Photocatalytic Degradation of Methyl Violet Dye Using Calcium Carbonate Nanoparticles Synthesized by Precipitation Method. *Chettinad Health City Medical Journal*, *9*(1). https://doi.org/10.36503/chcmj9(1)-02

[19] Satishkumar, P., Isloor, A. M., & Farnood, R. (2023). Expansive Applications of Chitosan and Its Derivatives in Membrane Technology. In

Handbook of Membrane Separations (3rd ed.). CRC Press.

[20] Syed Ibrahim, G. P., Isloor, A. M., Ismail, A. F., & Farnood, R. (2020). One-step synthesis of zwitterionic graphene oxide nanohybrid: Application to polysulfone tight ultrafiltration hollow fiber membrane. *Scientific Reports*, *10*(1), 6880. https://doi.org/10.1038/s41598-020-63356-2

[21] Bai, Chengling., Gu, Zhengyang., Ping Li, Ping., Ning, Rongsheng., & Yu, Shuili. (2024). A novel salt-swelling nanofiltration membranes for drinking water purification: High mineral ions passage and efficient organic removal. (2024). *Journal of the Taiwan Institute of Chemical Engineers*, *159*, 105473. https://doi.org/10.1016/j.jtice.2024.105473

[22] Isloor, A. M., Nayak, M. C., Inamuddin, Prabhu, B., Ismail, N., Ismail, A. F., & Asiri, A. M. (2019). Novel polyphenylsulfone (PPSU)/nano tin oxide (SnO_2) mixed matrix ultrafiltration hollow fiber membranes: Fabrication, characterization and toxic dyes removal from aqueous solutions. *Reactive and Functional Polymers*, *139*, 170–180. https://doi.org/10.1016/j.reactfunctpolym.2019.02.015

[23] Pereira, V. R., Isloor, A. M., Bhat, U. K., & Ismail, A. F. (2014). Preparation and antifouling properties of PVDF ultrafiltration membranes with polyaniline (PANI) nanofibers and hydrolysed PSMA (H-PSMA) as additives. *Desalination*, *351*, 220–227. https://doi.org/10.1016/j.desal.2014.08.002

[24] Zaman, N. K., Rohani, R., Mohammad, A. W., & Isloor, A. M. (2018). Polyimide-graphene oxide nanofiltration membrane: Characterizations and application in enhanced high concentration salt removal. *Chemical Engineering Science*, *177*, 218–233. https://doi.org/10.1016/j.ces.2017.11.034

[25] Ibrahim, G. P. S., Isloor, A. M., Inamuddin, Asiri, A. M., Ismail, A. F., Kumar, R., & Ahamed, M. I. (2018). Performance intensification of the polysulfone ultrafiltration membrane by blending with copolymer encompassing novel derivative of poly(styrene-co-maleic anhydride) for heavy metal removal from wastewater. *Chemical Engineering Journal*, *353*, 425–435. https://doi.org/10.1016/j.cej.2018.07.098

[26] Satishkumar, P., Isloor, A. M., & Farnood, R. (2023). Nanocomposite Membranes for Proton Exchange Membrane Fuel Cells. In *Proton Exchange Membrane Fuel Cells* (pp. 73–110). John Wiley & Sons, Ltd. https://doi.org/10.1002/9781119829553.ch5

[27] Kumar, R., Isloor, A. M., Ismail, A. F., Rashid, S. A., & Ahmed, A. A. (2013). Permeation, antifouling and desalination performance of TiO_2 nanotube incorporated PSf/CS blend membranes. *Desalination*, *316*, 76–84. https://doi.org/10.1016/j.desal.2013.01.032

[28] Nair, A. K., Isloor, A. M., Kumar, R., & Ismail, A. F. (2013). Antifouling and performance enhancement of polysulfone ultrafiltration membranes using $CaCO_3$ nanoparticles. *Desalination*, *322*, 69–75. https://doi.org/10.1016/j.desal.2013.04.031

[29] One-step synthesis of freestanding and translucent ZrO2 nanotube membranes by direct electrochemical anodization. (2024). *Materials Letters*, *368*, 136635. https://doi.org/10.1016/j.matlet.2024.136635

[30] Fabrication and oil-water separation properties of cerium oxide coated zirconium oxide composite membranes. (2024). *Colloids and Surfaces A: Physicochemical and Engineering Aspects*, *683*, 133069. https://doi.org/10.1016/j.colsurfa.2023.133069

[31] Ibrahim, G. P. S., Isloor, A. M., Inamuddin, Asiri, A. M., & Farnood, R. (2020). Tuning the surface properties of Fe_3O_4 by zwitterionic sulfobetaine: application to antifouling and dye removal membrane. *International Journal of Environmental Science and Technology*, *17*(9), 4047–4060. https://doi.org/10.1007/s13762-020-02730-z

[32] Bünger, L., Kurtz, T., Garbev, K., Stemmermann, P., & Stapf, D. (2024, June 7). Mixed Matrix Organo-Silica-Hydrotalcite Membrane for CO_2 Separation Part 2: Permeation and Selectivity Study. Preprints. https://doi.org/10.20944/preprints202406.0360.v1

[33] Fabrication of mesoporous TiO_2/PVDF photocatalytic membranes for efficient

photocatalytic degradation of synthetic dyes. (2021). *Journal of Environmental Chemical Engineering*, *9*(4), 105776. https://doi.org/10.1016/j.jece.2021.105776

[34] Tahiri Alaoui, O., Nguyen, Q. T., Mbareck, C., & Rhlalou, T. (2009). Elaboration and study of poly(vinylidene fluoride)–anatase TiO2 composite membranes in photocatalytic degradation of dyes. *Applied Catalysis A: General*, *358*(1), 13–20. https://doi.org/10.1016/j.apcata.2009.01.032

[35] Gnanaprakasam, A., Sivakumar, V. M., Sivayogavalli, P. L., & Thirumarimurugan, M. (2015). Characterization of TiO_2 and ZnO nanoparticles and their applications in photocatalytic degradation of azodyes. *Green Technologies for Environmental Pollution Control and Prevention (Part 1)*, *121*, 121–125. https://doi.org/10.1016/j.ecoenv.2015.04.043

[36] Poulios, I., & Tsachpinis, I. (1999). Photodegradation of the textile dye Reactive Black 5 in the presence of semiconducting oxides. *Journal of Chemical Technology & Biotechnology*, *74*(4), 349–357. https://doi.org/10.1002/(SICI)1097-4660(199904)74:4<349::AID-JCTB5>3.0.CO;2-7

How to site this paper:

Sneha, O., Isloor, A. M., Martis, G. J., Satishkumar, P. & Mugali, P. S. (2024). Impact of TiO_2 and $CaCO_3$ nanoparticles and their incorporation in polysulfone composite membrane on photocatalytic degradation of RB 5. Advances in Environmental Technology, 10(4), 315-325. doi: 10.22104/aet.2024.6957.1907